Journal of Hazardous Materials 318 (2016) 1–8

Contents lists available at ScienceDirect

Journal of Hazardous Materials

journal homepage: www.elsevier.com/locate/jhazmat

Mn-Promoted Co_3O_4/TiO_2 as an efficient catalyst for catalytic oxidation of dibromomethane (CH_2Br_2)

Jian Mei, Songjian Zhao, Wenjun Huang, Zan Qu, Naiqiang Yan*

School of Environmental Science and Engineering, Shanghai Jiao Tong University, 800 Dong Chuan Road, Shanghai, 200240, PR China

HIGHLIGHTS

- Mn(1)-Co/TiO_2 catalyst exhibited a good catalytic performance for DBM oxidation.
- The redox cycle ($Co^{2+} + Mn^{4+} \leftrightarrow Co^{3+} + Mn^{3+}$) existed over Mn(1)-Co/$TiO_2$ catalyst improved the redox property of the catalyst.
- The reaction mechanism for catalytic oxidation of DBM over Mn-Co/TiO_2 catalysts was proposed.

GRAPHICAL ABSTRACT

A plausible reaction mechanism for DBM oxidation over Mn-Co/TiO_2 catalysts.

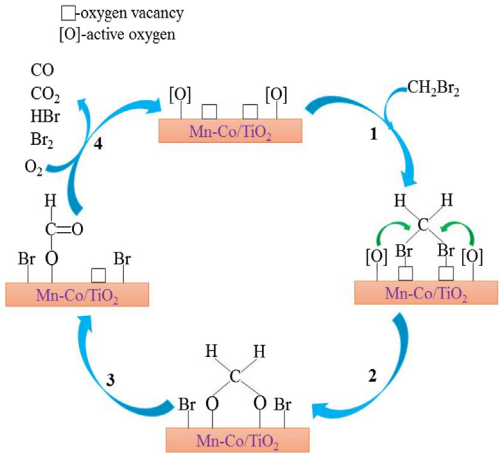

ARTICLE INFO

Article history:
Received 17 March 2016
Received in revised form 3 June 2016
Accepted 5 June 2016
Available online 6 June 2016

Keywords:
Catalytic oxidation
Dibromomethane
Cobalt
Manganese
In situ DRIFT

ABSTRACT

Brominated hydrocarbon is the typical pollutant in the exhaust gas from the synthesis process of Purified Terephthalic Acid (PTA), which may cause various environmental problems once emitted into atmosphere. Dibromomethane (DBM) was employed as the model compound in this study, and a series of TiO_2-supported manganese and cobalt oxide catalysts with different Mn/Co molar ratio were prepared by the impregnation method and used for catalytic oxidation of DBM. It was found that the addition of Mn significantly enhanced the catalytic performance of Co/TiO_2 catalyst. Among all the prepared catalysts, Mn(1)-Co/TiO_2 (Mn/Co molar ratio was 1) catalyst exhibited the highest activity with T_{90} at about 325 °C and good stability maintained for at least 30 h at 500 ppm DBM and 10% O_2 at GHSV = 60,000 h^{-1}, and the final products in the reaction were CO_x, HBr and Br_2, without the formation of Br-containing organics. The high activity and high stability might be attributed to the redox cycle ($Co^{2+} + Mn^{4+} \leftrightarrow Co^{3+} + Mn^{3+}$) over Mn-promoted Co_3O_4/TiO_2 catalyst. Based on the results of in situ DRIFT studies and analysis of products, a plausible reaction mechanism for catalytic oxidation of DBM over Mn-Co/TiO_2 catalysts was also proposed.

1. Introduction

Volatile organic compounds (VOCs) in exhaust gas emitted from various industrial processes and incineration of medical wastes are

* Corresponding author.
E-mail address: nqyan@sjtu.edu.cn (N. Yan).

http://dx.doi.org/10.1016/j.jhazmat.2016.06.010
0304-3894/

the major air pollutes. In particular, the release of purified terephthalic acid (PTA) exhaust gas has received much attention due to the potential environmental problems [1], and the incidents of the masses protesting against such projects have been occurred in China in recent years. The untreated PTA exhaust gas is a mixture of various organic components, including *p*-xylene (PX), acetic acid methyl ester and brominated hydrocarbon, which are harmful to the environment and human health [2]. At present, a great number of methods have been designed and used to treat the PTA exhaust gas, including activated carbon adsorption, thermal oxidation and catalytic oxidation. It is believed that catalytic oxidation is one of the most promising technologies due to lower operating temperature and the less secondary pollution products [1]. However, the catalyst should keep the ability of resisting bromine poisoning due to the presence of brominated hydrocarbon. Hence, the core issue of this technology is in search of high performance catalysts on the removal of brominated hydrocarbon.

In the past decades, many catalysts for catalytic oxidation of brominated hydrocarbon have been reported. But they were mainly focused on two types of catalysts, including the noble metal catalysts [3,4] and transition metal oxide catalysts [5–7]. Although the activity of noble metal catalysts was very high, the high cost and the easy deactivation by bromine poisoning prevented their applications on industries. Generally, the transition metal oxide catalysts were less active than the noble metal catalysts, but they could resist deactivation by bromine poisoning to a larger extent. Moreover, the transition metal oxide catalysts were cheaper. Therefore, it is of great interest to develop transition metal oxide catalysts with high catalytic activity and resistance to bromine poisoning.

As a typical transition metal oxide, cobalt oxides have been found to have a good performance for VOCs oxidation [8,9]. It is reported that cobalt oxides have the good redox ability due to the interconvert between Co^{2+} and Co^{3+} oxidation states, and the presence of Co_3O_4 means high catalytic activity for oxidation reaction [10]. When metal oxides are supported on TiO_2, there is often a strong metal-support interaction [11]. A TiO_2-supported Co-based catalyst prepared by the impregnation method could achieve high specific surface areas and promote the dispersion of active components, resulting in high catalytic activity. To our knowledge, appropriate modifications of the catalyst can further improve the catalytic activity and stability. Manganese oxides contain various valence states, which is significant to complete the catalytic cycle by redox mechanism. The Mn-Co/TiO_2 catalysts are highly effective low temperature SCR catalysts and have been widely studied [12–14]. However, no study on the behavior of Mn-Co/TiO_2 catalysts in the catalytic oxidation of brominated VOCs has been reported.

In this study, a series of Mn-Co/TiO_2 catalysts with various Mn/Co molar ratios were prepared by the impregnation method, and used in catalytic oxidation of dibromomethane (DBM) chosen as the model compound of brominated hydrocarbon. The structure and surface chemical properties of the catalysts were characterized by XRD, BET, Raman, H_2-TPR and XPS. The DBM conversion, analysis of products, products selectivity and catalyst stability were also investigated. Moreover, the in situ DRIFT analysis could further deepen our understanding of the promotional effect of Mn modified Co/TiO_2 catalyst on DBM oxidation.

2. Experimental section

2.1. Catalyst preparation and characterization

The Co/TiO_2, Mn/TiO_2 and Mn-Co/TiO_2 catalysts with various Mn/Co molar ratios were prepared by the impregnation method. In a typical synthesis, 25 mL of the aqueous precursor solution of $Co(NO_3)_3$ and $Mn(NO_3)_2$ was added into 50 mL beaker containing 2.0 g P25 TiO_2. The mixture was stirred for 4 h, dried at 60 °C overnight, and then clained at 500 °C for 3 h to get the desired catalyst. The cobalt loading was selected at 5 wt%, and the Mn/Co molar ratios were 0.2, 1, 2 and 3. The catalysts were donated as Mn(x)-Co/TiO_2, where x represents the molar ratio of Mn/Co. For comparison, 5 wt% Co_3O_4/TiO_2 (Co/TiO_2) and 5 wt% MnO_x/TiO_2 (Mn/TiO_2) catalysts were also prepared by the same method. The catalysts were characterized by XRD, BET, Raman, H_2-TPR and XPS, and the detail information was shown in supporting information.

2.2. Catalytic activity evaluation

The catalytic activity evaluation was carried out in a fixed-bed quartz reactor using 120 mg catalysts of 40–60 mesh. The feed gas mixture contained 500 ppm DBM, 10% O_2, 0 or 1% H_2O, 0 or 500 ppm *p*-xylene (PX), and N_2 as the balance gas. Water vapor was generated by passing N_2 through a heated gas-wash bottle containing deionized water. The total flow of the feed gas was 150 mL/min, corresponding to a gas hourly space velocity (GHSV) of 60,000 h^{-1}. The reaction was run from 150 to 450 °C in a step mode with a 20 min plateau at each temperature investigated. All the reactions were repeated three times to assure reproducibility and ruled out catalyst deactivation. The inlet and outlet DBM concentration was measured with a gas chromatograph (GC-9790) equipped with a FID detector. The removal efficiency of DBM was defined as:

$$\eta = \frac{C_0 - C}{C_0} \times 100\% \quad (1)$$

where C_0 and C were the inlet and outlet DBM concentrations, respectively. The gas products were detected by a gas chromatography and mass spectrometry (GCMS-QP2010, Shimadzu). The final products CO and CO_2 were measured using a gas chromatograph (GC-14B, Shimadzu) equipped with a FID detector with methane conversion oven. Br_2 and HBr were absorbed in a KI solution firstly. Then, Br_2 concentration was determined by the titration with sodium thiosulfate using starch solution as an indicator. The concentration of bromide ions in the bubbled solution was determined by using an ion chromatography. The selectivity of CO, CO_2, Br_2 and HBr was defined as, respectively:

$$S_{CO} = \frac{[CO]}{[C_T]} \times 100\% \quad (2)$$

$$S_{CO_2} = \frac{[CO_2]}{[C_T]} \times 100\% \quad (3)$$

$$S_{Br_2} = \frac{[Br_2]}{[C_{Br}]} \times 100\% \quad (4)$$

$$S_{HBr} = \frac{[HBr]}{[C_{Br}]} \times 100\% \quad (5)$$

where [CO] and [CO_2] were the amount of CO and CO_2 (ppm) after the reaction, [C_T] was the amount of carbon atom (ppm) in oxidized DBM during the reaction, which could be calculated by equation (6):

$$[C_T] = ([CH_2Br_2]_0 - [CH_2Br_2]) \quad (6)$$

where $[CH_2Br_2]_0$ and [CH_2Br_2] were the amount of DBM (ppm) in the gas stream before and after the reaction, respectively. [Br_2] and [HBr] were the amount of Br_2 and HBr (ppm) after the reaction, [C_{Br}] was the amount of bromine atom (ppm) in oxidized DBM during the reaction, which could be calculated by equation (7):

$$[C_{Br}] = ([CH_2Br_2]_0 - [CH_2Br_2]) \times 2 \quad (7)$$

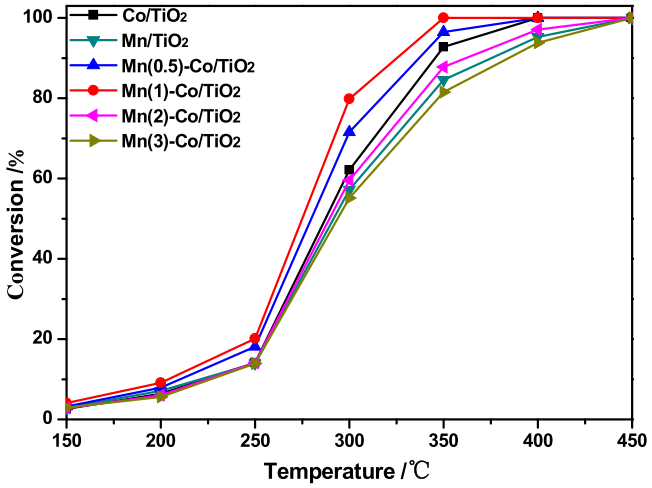

Fig. 1. The conversion curves for DBM oxidation over Co/TiO_2, Mn/TiO_2 and Mn(x)-Co/TiO_2 catalysts, where x = 0.2, 1, 2 and 3, respectively.

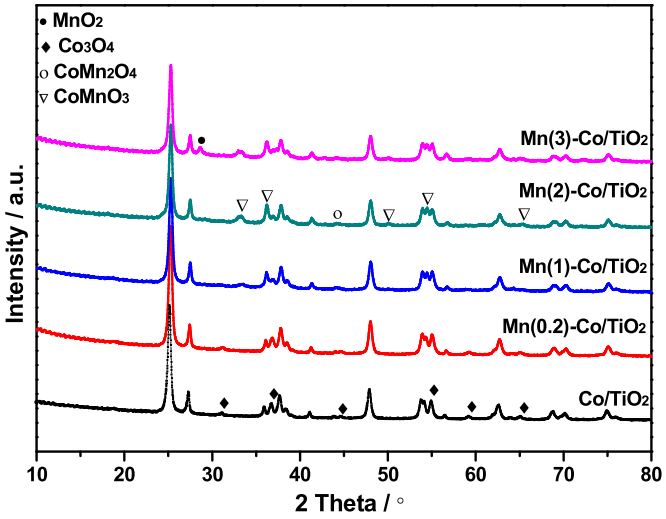

Fig. 2. XRD patterns of Co/TiO_2 and Mn(x)-Co/TiO_2 catalysts, where x = 0.2, 1, 2 and 3, respectively.

2.3. *In situ DRIFT studies*

In situ DRIFT spectra were recorded on a Fourier transform infrared spectrometer (FTIR, Nicolet 6700) equipped with a smart collector and an MCT detector cooled by liquid N_2. The DRIFT measurements were carried out in a high-temperature cell with ZnSe windows. Mass flow controllers and a sample temperature controller were used to simulate the real reaction conditions. In situ DRIFT spectra were recorded by accumulating 100 scans at a resolution of 4 cm^{-1}. Prior to each experiment, all the samples were pretreated with 10% O_2/N_2 at 400 °C for 2 h. Spectra of the clean catalyst surface were collected and used as the background at different temperature. Then, a 500 ppm DBM/10% O_2/N_2 stream was introduced into the IR cell at 50 °C for 1 h. Subsequently, the catalyst was treated in flowing 10% O_2/N_2 at different temperature. In situ DRIFT spectra were collected at different temperature when a steady was reached.

3. Results and discussion

3.1. *Catalytic performance*

The effect of adding Mn on the catalytic performance of Co/TiO_2 catalyst is shown in Fig. 1. As can be seen, Co/TiO_2 catalyst showed a considerable activity for DBM oxidation with T_{50} and T_{90} (the temperature needed for 50% and 90% conversion) of 288 °C and 346 °C, respectively. With the addition of Mn, the catalytic activity was improved and the conversion curves shifted to low temperature, T_{90} decreased to 337 °C for Mn(0.2)-Co/TiO_2 catalyst and to 325 °C for Mn(1)-Co/TiO_2 catalyst, respectively, indicating that the addition of Mn was beneficial for DBM oxidation. However, further increasing Mn loading leaded to a decrease of the catalytic activity, and T_{90} rose to 364 °C for Mn(2)-Co/TiO_2 catalyst and to 381 °C for Mn(3)-Co/TiO_2 catalyst, respectively. Therefore, the optimum Mn/Co ratio was 1. Moreover, Mn(1)-Co/TiO_2 catalyst was also more active than Mn/TiO_2 catalyst in the whole temperature range investigated.

3.2. *Catalyst characterization*

Fig. 2 shows the XRD patterns of Co/TiO_2 and Mn-Co/TiO_2 catalysts. As can be seen, TiO_2 existed in the form of anatase and rutile in all the prepared catalysts. In the pattern of Co/TiO_2 catalyst, very weak diffraction peaks were observed at 2 θ values of

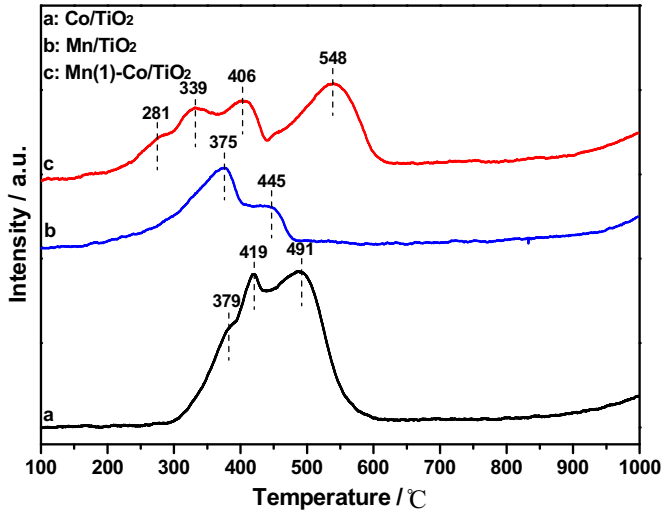

Fig. 3. H_2-TPR profiles of Co/TiO_2, Mn/TiO_2 and Mn(1)-Co/TiO_2 catalysts.

31.3°, 36.9°, 44.9°, 55.7°, 59.4° and 65.3°, which could be attributed to Co_3O_4 spinal structure (JPCDS: 76-1802) [15]. These peaks were very weak, which indicated that Co_3O_4 was low content or well dispersed on the TiO_2 support. For Mn-Co/TiO_2 catalysts, when the ratio of Mn/Co was 0.2 and 1, only the peaks attributed to TiO_2 and Co_3O_4 were observed. However, when the ratio of Mn/Co was 2 or higher, six new weak peaks at 33.5°, 36.4°, 50.3°, 54.8°, 65.5° and 44.2° were observed. The former five peaks were attributed to $CoMnO_3$ (JCPDS#12-0476) and the latter one was correspond to $CoMn_2O_4$ (PDF#01-1126), which demonstrated that two types of Co-Mn composite oxides were formed on the surface of TiO_2 support. These peaks were also weak, implying that the binary mental oxides were low content or high dispersed. In addition, when the ratio of Mn/Co was 3, a new peak at 28.8° of MnO_2 (JCPDS#44-0141) was also observed.

The H_2-TPR profiles of Co/TiO_2, Mn/TiO_2 and Mn(1)-Co/TiO_2 catalysts are shown in Fig. 3. As seen in Fig. 3, for Co/TiO_2 catalyst, there were three reduction peaks at 379, 419 and 491 °C. The first peak was attributed to the reduction of some surface oxygen, and the second and third peaks were ascribed to the reduction of Co^{3+} to Co^{2+} and Co^{2+} to Co^0, respectively [15]. In the case of Mn/TiO_2 catalyst, there were two reduction peaks at 375 and 445 °C. Accord-

Table 1
Relative atomic concentration on the catalyst surface.

Catalyst	Co^{3+}/Co	Mn^{4+}/Mn	O_{ads}/O
Co/TiO_2	56.9%	–	43.2%
$Mn(1)\text{-}Co/TiO_2$	100.0%	17.1%	49.4%
$Mn(1)\text{-}Co/TiO_2$ (used)	40.2%	32.3%	37.5%

ing to the results reported previously, the lower temperature peak was attributed to the reduction of Mn^{4+} to Mn^{3+}, and the higher temperature peak was corresponded to the reduction of Mn^{3+} to Mn^{2+} [16]. Moreover, the TPR profile of $Mn(1)\text{-}Co/TiO_2$ showed four reduction peaks located at 281, 339, 406 and 548 °C. It was noticed that these peaks were not only the simple combination of Co/TiO_2 and Mn/TiO_2 catalysts. According to the results of XRD, the Mn-Co mixed oxides existed in $Mn\text{-}Co/TiO_2$ catalyst. As can be seen, the first peak at 281 °C was far lower than the first reduction peak of Co/TiO_2 or Mn/TiO_2 catalyst due to an interaction between Co and Mn oxides. According to the literature reported [13], the first reduction peak could be due to the reduction of compound Co_3O_4•$CoMnO_3$, which might be the reason why Mn doping into Co/TiO_2 catalyst could lower the reduction peak temperature. The second and third reduction peaks located at 339 and 406 °C were also lower than these of Co/TiO_2 catalyst, which were attributed to the reduction of $CoMn_2O_4$ and CoO•MnO, respectively. Finally, the fourth reduction peak was ascribed to the reduction of Co^{2+} to Co^0, and it shifted from 491 to 548 °C due to the interaction between Co and Mn oxides. Consequently, it was deduced that the interaction between Co and Mn oxides resulted in the lower reduction temperature, which was beneficial for DBM oxidation.

Fig. 4 shows the XPS spectra of Co/TiO_2, $Mn(1)\text{-}Co/TiO_2$ and $Mn(1)\text{-}Co/TiO_2$ (used) catalysts over the spectral regions of Co 2p, Mn 2p, O 1 s and Br 3d, and the data of XPS are summarized in Table 1. As shown in Fig. 4(a), for Co/TiO_2, $Mn(1)\text{-}Co/TiO_2$ and $Mn(1)\text{-}Co/TiO_2$ (used) catalysts, there were two main peaks corresponding to Co $2p_{3/2}$ and Co $2p_{1/2}$ at 779.9 ~ 781.3 and 795.1 ~ 797.2 eV, respectively, with satellite peaks. By performing a peak fitting deconvolution, the Co $2p_{3/2}$ spectra could be decomposed to two characteristic peaks centered at 780.8 and 782.9 eV for Co/TiO_2 catalyst, which were ascribed to Co^{3+} and Co^{2+}, respectively. With the adding of Mn into Co/TiO_2 catalyst, the characteristic peaks of Co 2p shifted slightly to the low binding energy, and the amount of high valence Co was increased due to the interaction between Co and Mn oxides, which was beneficial for DBM oxidation. After reaction for 30 h at 300 °C, the characteristic peaks of Co 2p shifted slightly to the high binding energy and the amount of high valence cobalt was decreased, which was due to Co^{3+} participating in the reaction.

Fig. 4(b) shows the Mn 2p XPS spectra of $Mn(1)\text{-}Co/TiO_2$ and $Mn(1)\text{-}Co/TiO_2$ (used) catalysts. For $Mn(1)\text{-}Co/TiO_2$ catalyst, the binding energies of Mn $2p_{3/2}$ and Mn $2p_{1/2}$ were located at 641.9 and 653.4 eV, respectively. The spectra of Mn $2p_{3/2}$ could be separated into three characteristic peaks: Mn^{2+} (641.1 eV), Mn^{3+} (642.6 eV) and Mn^{4+} (644.8 eV). It was obvious that Mn existed in the mixture of Mn^{2+}, Mn^{3+} and Mn^{4+} states. After reaction for 30 h at 300 °C, the characteristic peaks of Mn 2p shifted slightly to the high binding energy and Mn existed mainly in the form of high valence states (seen in Table 1). And an amount of Mn^{3+} was oxidized to Mn^{4+}, which was beneficial to generate electrophilic oxygen to further oxidize Co^{2+} to Co^{3+}.

The O 1 s XPS spectra of Co/TiO_2, $Mn(1)\text{-}Co/TiO_2$ and $Mn(1)\text{-}Co/TiO_2$ (used) catalysts are shown in Fig. 4(c). The asymmetrical O 1 s peak could be fitted into two components: one at BE = 529.2-530.1 eV and the other at BE = 530.6-531.6 eV, the former was assigned to the surface lattice oxygen (O_{lat}) species, whereas the latter was assigned to the surface adsorbed oxygen (O_{ads}) species

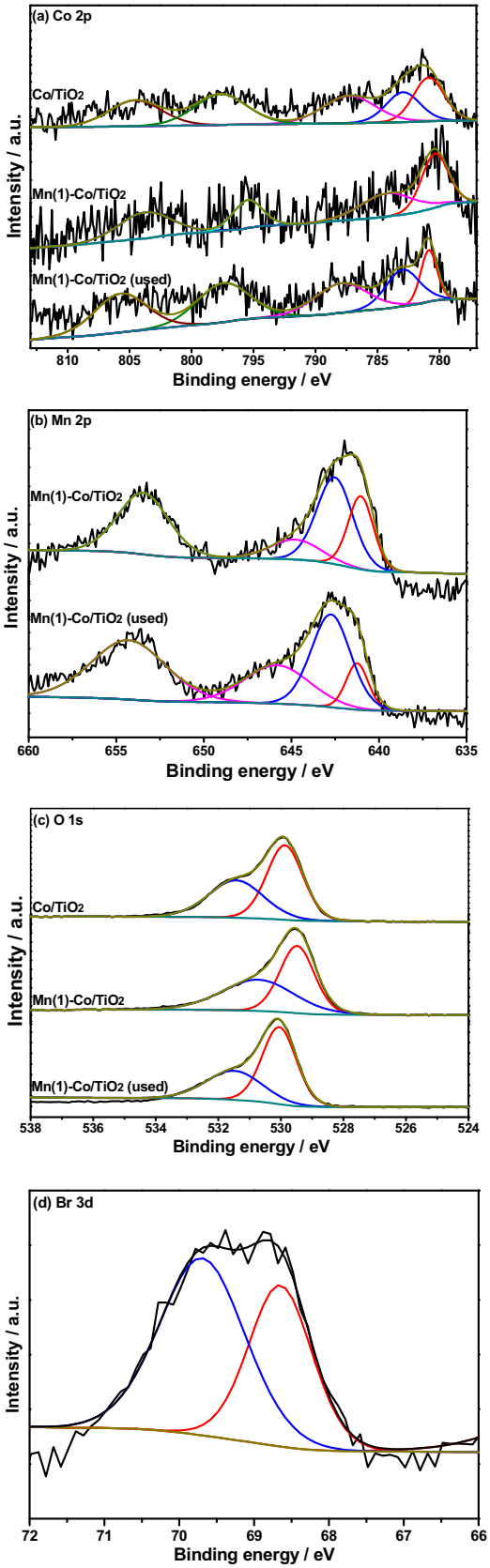

Fig. 4. XPS spectra of Co/TiO_2, $Mn(1)\text{-}Co/TiO_2$ and $Mn(1)\text{-}Co/TiO_2$ (used) over the spectral regions: (a) Co 2p, (b) Mn 2p, (c) O 1s, (d) Br 3d.

Table 2
Products in outlet at each evaluated temperature over Co/TiO_2 catalyst.

Temperature (°C)	Detected substances
150	CH_2Br_2, CH_2Br, CO, HBr, H_2O
200	CH_2Br_2, CH_2Br, CO, CO_2, HBr, H_2O
250	CH_2Br_2, CO, CO_2, HBr, H_2O
300	CH_2Br_2, CO, CO_2, HBr, H_2O
350	CH_2Br_2, CO, CO_2, HBr, Br_2, H_2O
400	CO, CO_2, HBr, Br_2, H_2O
450	CO, CO_2, HBr, Br_2, H_2O

Table 3
Products in outlet at each evaluated temperature over $Mn(1)\text{-}Co/TiO_2$ catalyst.

Temperature (°C)	Detected substances
150	CH_2Br_2, CO, HBr, H_2O
200	CH_2Br_2, CO, CO_2, HBr, H_2O
250	CH_2Br_2, CO, CO_2, HBr, H_2O
300	CH_2Br_2, CO, CO_2, HBr, Br_2, H_2O
350	CH_2Br_2, CO, CO_2, HBr, Br_2, H_2O
400	CO, CO_2, HBr, Br_2, H_2O
450	CO, CO_2, HBr, Br_2, H_2O

[17]. As seen in Table 1, it was evident that the proportion of surface adsorbed oxygen increased when adding Mn, which was beneficial for DBM oxidation. After reaction for 30 h at 300 °C, the amount of surface adsorbed oxygen decreased, suggesting that surface adsorbed oxygen participated in the reaction. However, surface adsorbed oxygen still existed on the catalyst surface, which might be due to the replenishment form lattice oxygen or gaseous oxygen.

The XPS Br 3d spectra of $Mn(1)\text{-}Co/TiO_2$ (used) catalyst is shown in Fig. 4(d). There were two peaks at 68.6 and 69.7 eV for Br 3d, which were attributed to the ionic (Br^-) and covalent (—Br) bromine species, respectively [18]. The ionic bromine (Br^-) might be the $CoBr_2$ generated by the reaction of the bromine species and cobalt, and the covalent (—Br) bromine species might be the adsorbed DBM.

3.3. Analysis of products

It is well known that the ideal decomposition products of brominated hydrocarbon are CO_2 and HBr or Br_2, however, almost all of the treatment technologies have a phenomenon of incomplete mineralization. In this study, the products in outlet at each evaluated temperature over Co/TiO_2 and $Mn(1)\text{-}Co/TiO_2$ catalysts were analyzed by GC–MS and the results were listed in Tables 2 and 3. As seen in Table 2, for Co/TiO_2 catalyst, the by-product CH_3Br was emerged at low temperature (below 200 °C) and it was disappeared with the increase of temperature. Br_2 was generated above 350 °C. With the addition of Mn into Co/TiO_2 catalyst, no other bromine by-products were generated and Br_2 was generated above 300 °C (seen in Table 3), which indicating that the doping of Mn into Co/TiO_2 catalyst could reduce the generation of bromine by-products and promote the generation of Br_2. Moreover, both Co/TiO_2 and $Mn(1)\text{-}Co/TiO_2$ catalysts, CO, HBr and H_2O were always existed at each evaluated temperature and CO_2 was generated above 200 °C.

Fig. 5 shows the DBM conversion and selectivity for CO, CO_2, HBr and Br_2 as a function of temperature over Co/TiO_2 (a) and $Mn(1)\text{-}Co/TiO_2$ (b) catalysts. It was found that the main products of DBM oxidation over Co/TiO_2 and $Mn(1)\text{-}Co/TiO_2$ catalysts were CO, CO_2 HBr and Br_2. However, their selectivity was different, depending on the catalysts used. For Co/TiO_2 catalyst, with the increase of temperature, the amount of CO_2 was gradually increased due to the further oxidation of CO, and its selectivity got to 50% when the temperature was 335 °C. When the temperature was above 350 °C, Br_2 was generated, which might be ascribed to the Deacon reaction ($4HBr + O_2 = 2Br_2 + 2H_2O$) [7]. With the further increase of

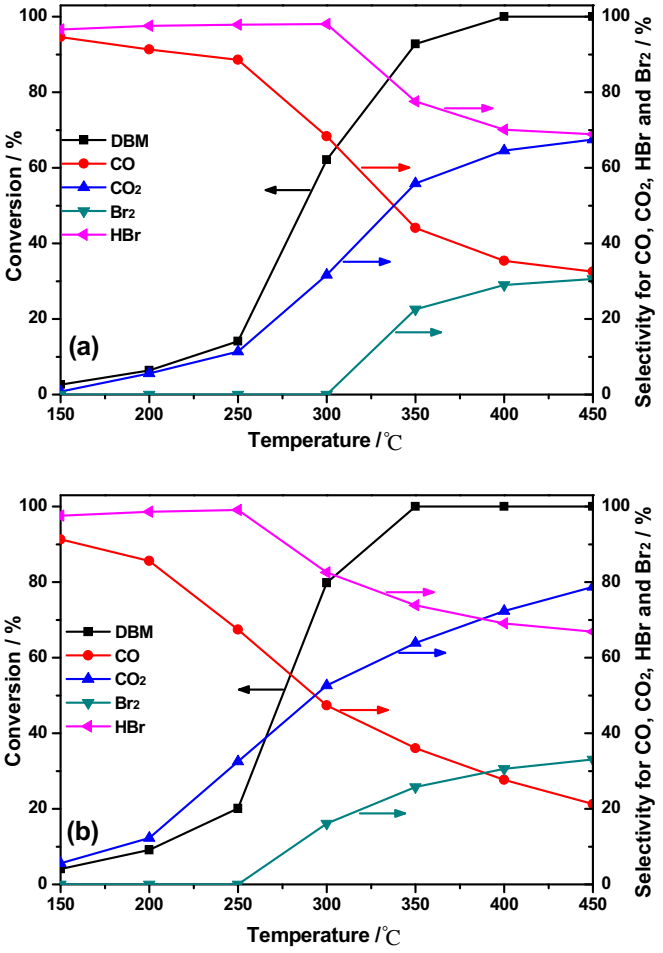

Fig. 5. DBM conversion and selectivity for CO, CO_2, HBr and Br_2 as a function of temperature over Co/TiO_2 (a) and $Mn(1)\text{-}Co/TiO_2$ (b) catalysts.

temperature, the selectivity for Br_2 was also further increased, and its selectivity got to 31% at 450 °C. For $Mn(1)\text{-}Co/TiO_2$ catalyst, it was found that the selectivity for CO_2 was higher than that of Co/TiO_2 catalyst at each temperature investigated, and its selectivity was exceeded 50% at 300 °C. Moreover, Br_2 was generated when the temperature was 300 °C, and the selectivity for Br_2 was also improved as the temperature increased, and its selectivity got to 34% at 450 °C. The results showed that the doping of Mn into Co/TiO_2 catalyst was beneficial for improving the redox properties of the catalyst, promoting the further oxidation of CO to CO_2 and the generation of Br_2.

3.4. The effect of water or p-xylene (PX)

It is necessary to investigate the effect of water on the activity of catalyst for DBM oxidation. As shown in Fig. 6, the DBM conversion curve over $Mn(1)\text{-}Co/TiO_2$ catalyst as a function of temperature was obtained in the presence of 1% (V/V) water. In the presence of water, the conversion of DBM was promoted at low temperature, and the temperature for 10% conversion decreased by about 20 °C. The most plausible explanation for the promoting effect of water on DBM oxidation at low temperature was the removal of surface bromine species, which was based on the reverse Deacon reaction: $H_2O + Br^- \leftrightharpoons HBr\uparrow + OH^-$ [19], and thus prevented catalyst deactivation. However, the decrease in activity was observed with the increase of temperature due to the adsorption of water on the active sites[19].

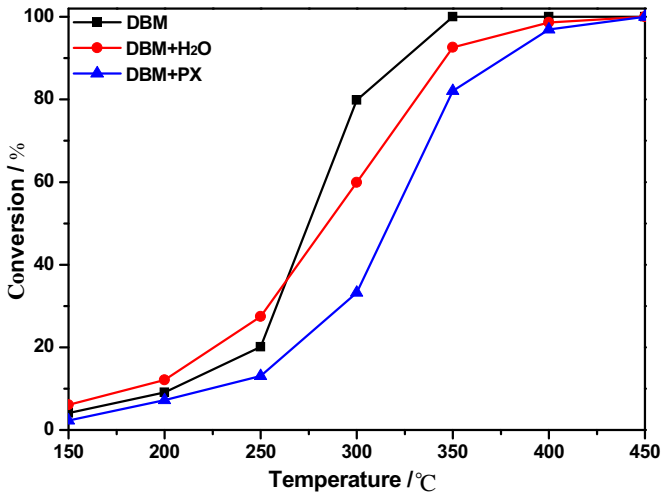

Fig. 6. The effect of water or *p*-xylene (PX) on DBM oxidation over Mn(1)-Co/TiO_2 catalyst; DBM alone: 500 ppm DBM; DBM + H_2O: 500 ppm DBM + 1% (V/V) H_2O; DBM + PX: 500 ppm DBM + 500 ppm PX.

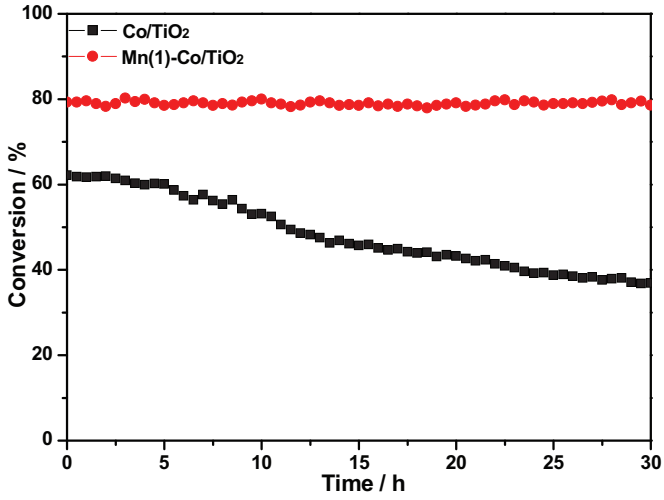

Fig. 7. The activity for DBM oxidation over Co/TiO_2 and Mn(1)-Co/TiO_2 catalysts on stream feed at 300 °C for 30 h.

It is known that there are all kinds of organic compounds in PTA exhaust gas, and these organic compounds will compete active sites during the catalytic reaction. Considering the complexity of actual exhaust gas, it is too unrealistic to study all the organic compounds at the same time. Therefore, we mainly concentrate on the reaction feature when the reaction system involves binary pollutants. As we all know, *p*-xylene (PX) is one of the major components in PTA exhaust gas. Hence, the effect of feeding *p*-xylene (PX) into the reaction mixture on the activity of Mn(1)-Co/TiO_2 catalyst was investigated. As seen in Fig. 6, in the presence of *p*-xylene (PX), the conversion of DBM was inhibited whether at low or high temperature, and T_{90} shifted to 378 °C, which was attributed to the consumption of surface active oxygen in *p*-xylene (PX) oxidation decreased oxygen species.

3.5. Catalyst stability

The stability of the catalyst was also evaluated by performing long catalytic time at constant oxidation temperature. The evolutions of DBM conversion with time on stream at 300 °C for Co/TiO_2 and Mn(1)-Co/TiO_2 catalysts are shown in Fig. 7. Within 30 h, the DBM conversion over Co/TiO_2 catalyst decreased from 62% to 37%, which might be attributed to the accumulation of Br species on the surface of Co/TiO_2 catalyst. XPS analysis showed 2.56% Br deposited on the surface of Co/TiO_2 catalyst after 30 h reaction. However, Mn(1)-Co/TiO_2 catalyst maintained its catalytic activity well within 30 h at 300 °C with the conversion at high as 79.6%. XPS analysis showed only 1.42% Br deposited on the surface of Mn(1)-Co/TiO_2 catalyst after 30 h reaction, which was lower than Co/TiO_2 catalyst. The results indicated that the presence of Mn promoted the removal of Br species on the catalyst surface.

3.6. In situ DRIFT studies

In order to further understand the catalytic behaviors of the catalyst surface, in situ DRIFT experiments were conducted on Co/TiO_2 and Mn(1)-Co/TiO_2 catalysts and the results are shown in Fig. 8. As seen in Fig. 8(a, b), for Co/TiO_2 catalyst, after introduction of 500 ppm DBM and 10% O_2 at 50 °C for 1 h, the DRIFT spectra showed the bands at 3072, 2992, 1600 and 1201 cm^{-1}. The bands at 3072, 2992 and 1201 cm^{-1} were ascribed to antisymmetric stretching, symmetric stretching and wagging of methylene, respectively, which were the approximate mode of DBM adsorbed molecules on the surface of Co/TiO_2 catalyst at 50 °C [20,21]. With the increase of temperature, the intensity of these bands diminished gradually and complete disappeared above 100 °C, indicating either consumption or desorption of DBM molecules. The band at 1600 cm^{-1} was ascribed to H_2O absorbed on the catalyst surface [22], which diminished gradually with the increase of temperature. Moreover, the disappearance of the bands ascribed to DBM was accompanied by appearance of the new bands of 2960, 2935, 2873, 2835, 1560, 1380, 1365 and 1215 cm^{-1}. The bands at 2960, 2873, 1560, 1380 and 1365 cm^{-1} (including 2881 cm^{-1} developed at 150 °C) were ascribed to the adsorbed formate species [23,24]. While the other bands at 2935 and 2835 cm^{-1} were ascribed to methyl antisymmetric stretching and symmetric stretching of the absorbed methoxy groups [25,26]. In addition, the band at 1215 cm^{-1} was generated at 250 °C, which was ascribed to bicarbonate [27]. All the bands developed with the absorbed DBM oxidation, indicating that the formate groups and methoxy groups were the main intermediate species generated on the surface of Co/TiO_2 catalyst.

For Mn(1)-Co/TiO_2 catalyst (Fig. 8(c, d)), it was evident that the intensities of the peaks attributed to adsorbed DBM were noticeably higher than those over Co/TiO_2 catalyst at 50 °C, and the DRIFT spectra of adsorbed species of DBM reaction at 50, 100, 150, 200 and 250 °C were similar to these of Co/TiO_2 catalyst, and expect for the bands ascribed to the methoxy groups were not appeared, meaning that the methoxy groups were not the intermediate species during the reaction, which was beneficial to reduce the generation of by-products, such as CH_3Br. In addition, the new bands at 1412 and 1346 cm^{-1} were ascribed to formate groups [23] and carbonate [28], respectively. The appearance of the band ascribed to carbonate indicated that the formate groups were further oxidized, which was beneficial for generation of more CO_2. With the increase of temperature, the intensity of all the bands decreased at 250 °C and basic disappeared at 300 °C. The results suggested that the presence of Mn further enhanced the degradation of intermediate species to CO and CO_2. Moreover, it was difficult to observe the bands ascribed to the formate groups above 300 °C. Furthermore, no bands ascribed to CO, CO_2 and HBr as final products could be observed due to the quick desorption of them.

In order to obtain a deeper understanding of this reaction, a plausible mechanism for DBM oxidation over Mn-Co/TiO_2 catalysts is shown in Fig. 9. This reaction pathway was ascribed as follows: (1) A DBM molecule adsorbed on oxygen vacancies of the catalyst surface through the two bromine atoms. (2) The two bromine atoms were abstracted by the adjacent nucleophilic oxygen, and

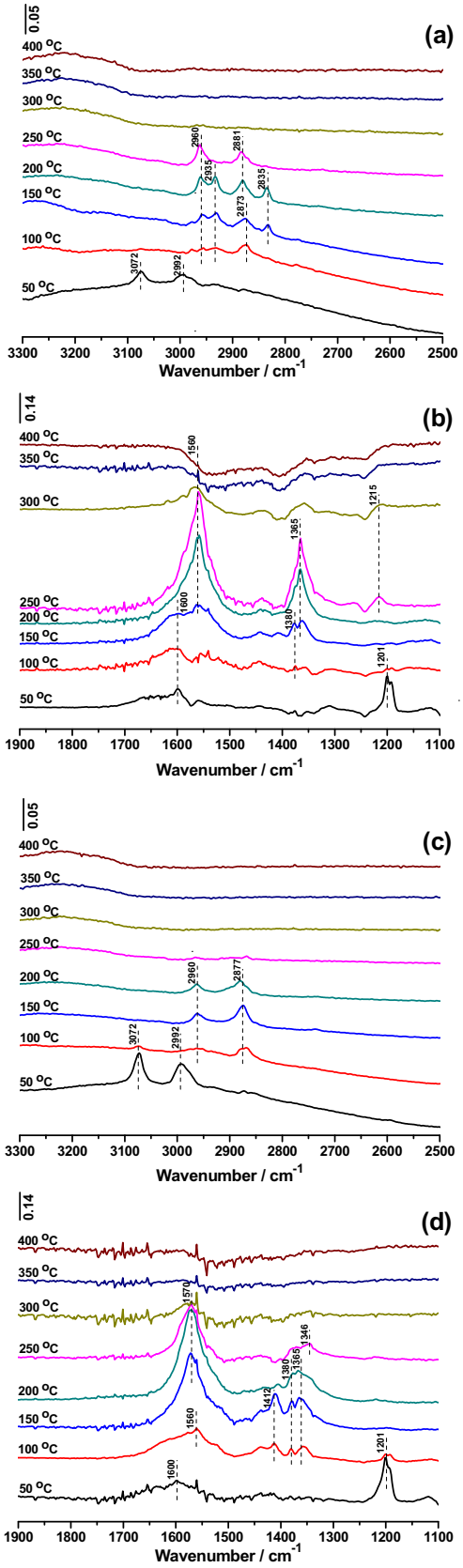

Fig. 8. In situ DRIFT spectra of DBM oxidation over Co/TiO_2 (a, b) and $Mn(1)\text{-}Co/TiO_2$ (c, d) catalysts at different temperature.

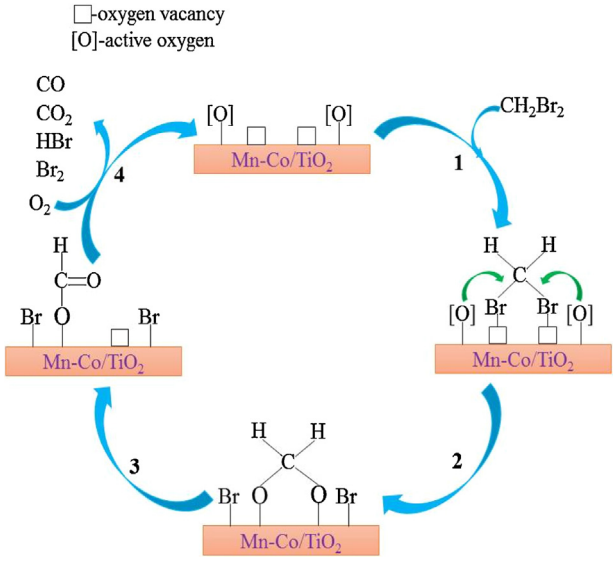

Fig. 9. A plausible mechanism for DBM oxidation over $Mn\text{-}Co/TiO_2$ catalysts.

generating the hemiacetal species [29]. (3) The adsorption of gas-phase oxygen on the surface oxygen vacancies to replenish the consumed oxygen. (4) The hemiacetal species were attacked to form the formate species. (5) The formate species were further oxidation by surface active oxygen species to form CO and CO_2. Under oxygen-rich condition, the Br species could react with the surface hydroxyl groups to form HBr or aggregated to generate Br_2. Moreover, it was possible that Br_2 was generated via the Deacon reaction ($4HBr + O_2 = 2Br_2 + 2H_2O$).

It is well known that the redox properties are the important factors controlling the reactivity of the catalysts. Based on the XPS results, it can be seen that a high ratio Mn^{3+} (51.6%) exists over $Mn(1)\text{-}Co/TiO_2$ catalyst. Combining with the H_2-TPR results, the existence of Mn^{3+} could contribute to the redox process of Co^{2+}/Co^{3+}. Thus, the redox cycle ($Co^{2+} + Mn^{4+} \leftrightarrow Co^{3+} + Mn^{3+}$) existed over $Mn(1)\text{-}Co/TiO_2$ catalyst and the electron transfer could be facilitated as follows: $Mn^{4+} - O^{2-} - Co^{3+} + e \leftrightarrow Mn^{4+} - O^{2-} - Co^{2+} \leftrightarrow Mn^{3+} - O^{2-} - Co^{3+} \leftrightarrow Mn^{4+} - O^{2-} - Co^{3+} + e$. The redox cycle leaded to a decrease in the energy required for the electron transfer between Mn and Co active sites, promoting the adsorption of DBM. In addition, the presence of Mn induced the formation of more surface oxygen species, which was also beneficial for DBM oxidation. Thus, $Mn(1)\text{-}Co/TiO_2$ catalyst exhibited higher catalytic performance than Co/TiO_2 catalyst for DBM oxidation.

4. Conclusion

In this study, a series of $Mn\text{-}Co/TiO_2$ catalysts were prepared by the impregnation method, and used in catalytic oxidation of DBM chosen as the model compound of brominated hydrocarbon. $Mn(1)\text{-}Co/TiO_2$ catalyst exhibited the highest catalytic activity with T_{90} of 325 °C, and the DBM removal activity remained without any appreciable deactivation for 30 h long-time stability at 300 °C, which suggested the presence of Mn promoted the stable activity of Co/TiO_2 catalyst through retarding the exchange of bromide for basic lattice oxygen or surface hydroxyl groups. The enhanced performance resulted from the existing redox cycle ($Co^{2+} + Mn^{4+} \leftrightarrow Co^{3+} + Mn^{3+}$). The in situ DRIFT studies revealed that the presence of Mn over $Mn(1)\text{-}Co/TiO_2$ catalyst could promote the adsorption of DBM and enhance the degradation of intermediate species. Finally, based on the results of in situ DRIFT studies and analysis of products, a plausible mechanism for DBM oxidation

over Mn-Co/TiO_2 catalysts was proposed. Firstly, BDM adsorbed on surface oxygen vacancies, then active oxygen attacked adsorption intermediates to form the formate groups, and finally further oxidation of the formate species to form CO and CO_2.

Acknowledgements

This work was supported by the Major State Basic Research Development Program of China (973 Program, No. 2013CB430005).

Appendix A. Supplementary data

Supplementary data associated with this article can be found, in the online version, at http://dx.doi.org/10.1016/j.jhazmat.2016.06.010.

References

[1] B. Chen, J. Carson, J. Gibson, R. Renneke, T. Tacke, M. Reisinger, R. Hausmann, A. Geisselmann, G. Stochniol, P. Panster, Destruction of PTA offgas by catalytic oxidation, CHEMICAL INDUSTRIES-NEW YORK-MARCEL DEKKER. (2003) 179–190.
[2] M. Moreton, Catalytic oxidation for PTA plant emissions control, Int. J. Hydrocarbon Eng. 3 (1998) 57–58.
[3] K. Ding, A.R. Derk, A. Zhang, Z. Hu, P. Stoimenov, G.D. Stucky, H. Metiu, E.W. McFarland, Hydrodebromination and oligomerization of dibromomethane, ACS Catal. 2 (2012) 479–486.
[4] X. Liu, J. Zeng, J. Wang, W. Shi, T. Zhu, Catalytic oxidation of methyl bromide using ruthenium-based catalysts, Catal. Sci. Technol. (2016).
[5] G.R. Lester, Catalytic destruction of hazardous halogenated organic chemicals, Catal. Today 53 (1999) 407–418.
[6] L. Feng-fen, C. Xian, T. Ji-hai, C. Mi-fen, Q. Xu, Catalytic performance of dibromomethane combustion over Ce-Mn mixed oxide, J. Nanjing Univ. Technol. 6 (2010).
[7] C.-Y. Chen, J.J. Pignatello, Catalytic oxidation for elimination of methyl bromide fumigation emissions using ceria-based catalysts, Appl. Catal. B: Environ. 142–143 (2013) 785–794.
[8] B. de Rivas, R. López-Fonseca, C. Jiménez-González, J.I. Gutiérrez-Ortiz, Synthesis, characterisation and catalytic performance of nanocrystalline Co_3O_4 for gas-phase chlorinated VOC abatement, J. Catal. 281 (2011) 88–97.
[9] H. Nguyen, S.A. El-Safty, Meso-and macroporous Co_3O_4 nanorods for effective VOC gas sensors, J. Phys. Chem. C 115 (2011) 8466–8474.
[10] L. Qiu, Y. Wang, D. Pang, F. Ouyang, C. Zhang, G. Cao, Characterization and catalytic activity of Mn-Co/TiO_2 catalysts for NO oxidation to NO_2 at low temperature, Catalysts 6 (2016) 9.
[11] C.-H. Lin, J.-H. Chao, C.-H. Liu, J.-C. Chang, F.-C. Wang, Effect of calcination temperature on the structure of a Pt/TiO_2(B) nanofiber and its photocatalytic activity in generating H_2, Langmuir 24 (2008) 9907–9915.
[12] H. Hu, S. Cai, H. Li, L. Huang, L. Shi, D. Zhang, Mechanistic aspects of deNO_x processing over TiO_2 supported Co–Mn oxide catalysts: structure–Activity relationships and In situ DRIFTs analysis, ACS Catal. 5 (2015) 6069–6077.
[13] L. Qiu, J. Meng, D. Pang, C. Zhang, F. Ouyang, Reaction and characterization of Co and Ce doped Mn/TiO_2 catalysts for low-temperature SCR of NO with NH_3, Catal. Lett. 145 (2015) 1500–1509.
[14] H. Hu, J.L. Xie, D. Fang, F. He, Study of Co-Mn/TiO_2 SCR catalyst at low temperature, in: Advanced Materials Research, Trans. Tech. Publ., 2015, pp. 11–16.
[15] Q. Wang, Y. Peng, J. Fu, G.Z. Kyzas, S.M.R. Billah, S. An, Synthesis, characterization, and catalytic evaluation of Co_3O_4/γ-Al_2O_3 as methane combustion catalysts: significance of Co species and the redox cycle, Appl. Catal. B: Environ. 168–169 (2015) 42–50.
[16] F. Wang, H. Dai, J. Deng, G. Bai, K. Ji, Y. Liu, Manganese oxides with rod-, wire-, tube-, and flower-like morphologies: highly effective catalysts for the removal of toluene, Environ. Sci. Technol. 46 (2012) 4034–4041.
[17] J. Li, G. Lu, G. Wu, D. Mao, Y. Guo, Y. Wang, Y. Guo, Effect of TiO_2 crystal structure on the catalytic performance of Co_3O_4/TiO_2 catalyst for low-temperature CO oxidation, Catal. Sci. Technol. 4 (2014) 1268.
[18] S.A. Al-Bataineh, L.G. Britcher, H.J. Griesser, Rapid radiation degradation in the XPS analysis of antibacterial coatings of brominated furanones, Surf. Interface Anal. 38 (2006) 1512–1518.
[19] C.E. Hetrick, F. Patcas, M.D. Amiridis, Effect of water on the oxidation of dichlorobenzene over V_2 O_5/TiO_2 catalysts, Appl. Catal. B: Environ. 101 (2011) 622–628.
[20] M.-T. Chen, C.-F. Lien, L.-F. Liao, J.-L. Lin, In-situ FTIR study of adsorption and photoreactions of CH_2Cl_2 on powdered TiO_2, J. Phys. Chem. B 107 (2003) 3837–3843.
[21] F. Solymosi, J. Rasko, Infrared spectroscopic study of the adsorption and dissociation of CH_2Cl_2 on Pd/SiO_2 generation of CH_2 species, J. Catal. 155 (1995) 74–81.
[22] Y. Wang, A.-P. Jia, M.-F. Luo, J.-Q. Lu, Highly active spinel type $CoCr_2O_4$ catalysts for dichloromethane oxidation, Appl. Catal. B: Environ. 165 (2015) 477–486.
[23] C.-C. Chuang, W.-C. Wu, M.-C. Huang, I.-C. Huang, J.-L. Lin, FTIR study of adsorption and reactions of methyl formate on powdered TiO_2, J. Catal. 185 (1999) 423–434.
[24] C. Ma, D. Wang, W. Xue, B. Dou, H. Wang, Z. Hao, Investigation of formaldehyde oxidation over Co_3O_4-CeO_2 and Au/Co_3O_4-CeO_2 catalysts at room temperature: effective removal and determination of reaction mechanism, Environ. Sci. Technol. 45 (2011) 3628–3634.
[25] W.-C. Wu, C.-C. Chuang, J.-L. Lin, Bonding geometry and reactivity of methoxy and ethoxy groups adsorbed on powdered TiO_2, J. Phys. Chem. B 104 (2000) 8719–8724.
[26] C. Su, J.-C. Yeh, C.-C. Chen, J.-C. Lin, J.-L. Lin, Study of adsorption and reactions of methyl iodide on TiO_2, J. Catal. 194 (2000) 45–54.
[27] C.-W. Tang, L.-C. Hsu, S.-W. Yu, C.-B. Wang, S.-H. Chien, In situ FT-IR and TPD-MS study of carbon monoxide oxidation over a CeO_2/Co_3O_4 catalyst, Vib. Spectrosc. 65 (2013) 110–115.
[28] Z. Ren, Z. Wu, W. Song, W. Xiao, Y. Guo, J. Ding, S.L. Suib, P.-X. Gao, Low temperature propane oxidation over Co_3O_4 based nano-array catalysts: ni dopant effect, reaction mechanism and structural stability, Appl. Catal. B: Environ. 180 (2016) 150–160.
[29] I. Maupin, L. Pinard, J. Mijoin, P. Magnoux, Bifunctional mechanism of dichloromethane oxidation over Pt/Al_2O_3: CH_2Cl_2 disproportionation over alumina and oxidation over platinum, J. Catal. 291 (2012) 104–109.